Structure, Bonding, and Reactivity of the Organometallic 1,3,2,4-Dithiadiazole Complex $CpCoS_2N_2$

Joris Van Droogenbroeck,[†] Christian Van Alsenoy,[†] Stephen M. Aucott,[‡] J. Derek Woollins,[‡] Allen D. Hunter,[§] and Frank Blockhuys*,[†]

Department of Chemistry, University of Antwerp, Universiteitsplein 1, B-2610 Wilrijk, Belgium, Department of Chemistry, University of St. Andrews, St. Andrews KY16 9ST, United Kingdom, and Department of Chemistry, Youngstown State University, One University Plaza, Youngstown, Ohio 44555-3663

Received August 2, 2004

The bonding and spectroscopic properties of 5-(η^5-cyclopentadienyl)-5-cobalta-1,3,2,4-dithiadiazole (i.e., a structure having a Co−N−S−N−S five-membered ring, abbreviated $CpCoS_2N_2$) have been studied, based on the results of theoretical calculations at the DFT/B3LYP level with the 6-311+G* basis set and on a redetermination of the single-crystal structure and experimental NMR spectra. A description of the bonding is provided based on a combination of geometrical data, electron densities, bond orders, and valencies, and a critical evaluation of the aromaticity of the compound is given based on several aromaticity criteria. In addition, a dipole analysis is performed and the reactive sites in this complex are located by means of atomic charges, molecular electrostatic potentials, Fukui functions, and local softnesses.

1. Introduction

Main-group inorganic compounds are interesting both in their own right and for their applications to other areas of chemistry, including their use as ligands for transition metal complexes and catalysts,[1−5] as reagents for organic synthesis,[6−9] and as components of solid-state materials.[10−19] A central theme in these studies has been to explore the wide structural diversity and reactivities of these materials, especially their abilities to form complex rings and cages.[20−23] During the course of these studies, the community has developed a solid empirical understanding of many of these classes of compounds based on their observed physical, spectroscopic, and electronic properties, their reactivities, and their structures. Ideally, one would like to integrate all of this quantitative structure−property data in terms of a consistent bonding model that would allow the rational design of future materials having precisely tuned properties for each of these applications. Unfortunately, the compounds of interest for these applications typically have a minimum of a dozen atoms, including a transition metal atom and at least several heavier main-group atoms such as sulfur and/or phosphorus. Until recently, this meant that either one had to use higher-level theoretical approaches using basis sets that were known to be too small and with only poor corrections for correlation or one had to use semiempirical methods that are not theoretically rigorous and that often give less than satisfactory answers. In the last several years, a number of theoretical approaches have been validated that allow one to overcome these

* Corresponding author. Fax: +32.3.820.23.10. E-mail: frank.blockhuys@ua.ac.be.
[†] University of Antwerp.
[‡] University of St. Andrews.
[§] Youngstown State University.

(1) Atwood, J. D. *Inorganic and Organometallic Reaction Mechanisms*; VCH: New York, 1997.
(2) Finet, J. P. *Ligand Coupling Reactions with Heteroatomic Compounds*; Pergamon: New York, 1998.
(3) Russo, N.; Salahub, D. R. *Metal−Ligand Interactions: Structure and Reactivity*; Kluwer: Dordrecht, 1996.
(4) Jordan, R. B. *Reaction Mechanisms of Inorganic and Organometallic Systems*; Oxford University Press: New York, 1998.
(5) Figgis, B. N.; Hitchman, M. A. *Ligand Field Theory and its Applications*; John Wiley & Sons: New York, 2000.
(6) Hegedus, L. S. *Transition Metals in the Synthesis of Complex Organic Molecules*; University Science Books: Mill Valley, 1999.
(7) Collman, J. P.; Hegedus, L. S.; Norton, J. R.; Finke, R. G. *Principles and Applications of Organotransition Metal Chemistry*; University Science Books: Mill Valley, 1987.
(8) Constable, E. C. *Metals and Ligand Reactivity: an Introduction to the Organic Chemistry of Metal Complexes*; John Wiley & Sons: New York, 1996.
(9) Bateson, J. H.; Mitchell, M. B. *Organometallic Reagents in Organic Synthesis*; Academic Press: London, 1994.
(10) Buchanan, R. C.; Park, T. *Materials Crystal Chemistry*; Dekker: New York, 1997.
(11) Atwood, J. L.; Lehn, J. M. *Comprehensive Supramolecular Chemistry*; Pergamon: New York, 1996.
(12) Echegoyen, L.; Kaifer, A. E. *Physical Supramolecular Chemistry*; Kluwer: Dordrecht, 1996.
(13) Freiser, B. S. *Organometallic Ion Chemistry*. Kluwer: Dordrecht, 1996.
(14) Seddon, K. R.; Zaworotko, M. *Crystal Engineering: the Design and Application of Functional Solids*; Kluwer: Dordrecht, 1999.
(15) Scheiner, S. *Molecular Interactions: from Van der Waals to Strongly Bound Complexes*; John Wiley & Sons: New York, 1997.
(16) Rao, C. N. R. *New Directions in Solid State Chemistry*; Cambridge University Press: Cambridge, 1997.
(17) Winter, C. H., Hoffman, D. M., Eds. *Inorganic Materials Synthesis: New Directions for Advanced Materials*; American Chemical Society: Washington, DC, 1999.
(18) van der Put, P. J. *The Inorganic Chemistry of Materials: How to Make Things out of Elements*; Kluwer: Dordrecht, 1998.
(19) Jones, W. *Organic Molecular Solids: Properties and Applications*; CRC Press: Boca Raton, 1997.
(20) Massey, A. G. *Main Group Chemistry*; John Wiley & Sons: New York, 1990.
(21) King, R. B. *Inorganic Chemistry of Main Group Elements*; John Wiley & Sons: New York, 1995.
(22) Cowley, A. H. *Rings, Clusters, and Polymers of the Main Group Elements*; Oxford University Press: Oxford, 1983.
(23) *Specialist Periodical Reports: Inorganic Chemistry of the Main Group Elements*.

10.1021/om0494059 CCC: $30.25 © 2005 American Chemical Society
Publication on Web 02/02/2005

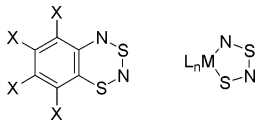

Figure 1. Representative 1,3$\lambda^4\delta^2$,2,4-benzodithiadiazines and 5,1,3,2,4-metalladithiadiazoles.

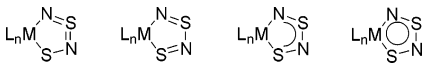

Figure 2. Representative selection of bonding models proposed for 5,1,3,2,4-metalladithiadiazoles.

limitations on real molecules having multiple 3p and/or 3d centers.[24−27] In particular, recent advances in density functional theory (DFT) allow one to study such complex real-world systems.

One family of such inorganic systems of interest are the compounds having one or more sulfur−nitrogen linkages. As the starting point of this project, we focused our interest on the dozens of known heterocyclic compounds having an NSNS sequence in a five- or six-membered ring (see Figure 1). This choice was made because it was known that apparently small changes to the other atoms in the ring and to their substituents caused large changes to the structure and bonding of the five- and six-membered rings. In particular, these rings display a very wide range of interatomic distances and other geometrical features such as planarity that could not be satisfactorily explained even in qualitative terms.

Building on the success of a number of collaborative efforts for a limited set of (in)organic NSNS ring systems,[28−31] we decided to study the more computationally challenging transition metal organometallic systems. In particular, inspection of the crystallographic data[32] that has been published for a number of monometallic and bi- and polymetallic L_nM(NSNS) complexes (i.e., where L_n are the ancillary ligands on the metal center and M = Co, Ir, Ni, Pd, Pt, etc.) indicated that, based primarily on bond length data derived from conventional single-crystal X-ray diffraction studies, multiple different bonding models for this heterocyclic ring had been proposed (Figure 2). In addition to these structural anomalies, other interesting trends were observed but not quantitatively explained. For example, inspection of the known structures indicates that hard electrophiles such as H^+ or R^+ always bind to N(4), while softer ones may also bind to N(2). It was to explain the origins of these empirical structure−property relationships that the current quantitative study was undertaken. In the current paper, a density functional study of the title complex is reported and the results of these calculations are related to data from single-crystal X-ray diffraction, spectroscopic techniques, and reactivity studies. To this day, only few studies of this compound have been undertaken.[33−35] The choice of the DFT methodology is based on its successful description of other NSNS-containing compounds[28,29] on one hand and on its successful description of organometallic compounds, especially when making use of hybrid functionals,[24−27] on the other.

2. Experimental Section

2.1. Synthesis and Spectroscopy. The 5-(η^5-cyclopentadienyl)-5-cobalta-1,3,2,4-dithiadiazole was synthesized by the literature method.[34] ^{1}H and ^{13}C NMR spectra were recorded at 25 °C on a JEOL DELTA GSX270 spectrometer in $CDCl_3$ with the chemical shift δ referenced to external tetramethylsilane (TMS).

2.2. X-ray Structure Determination. Crystal structure data for 5-(η^5-cyclopentadienyl)-5-cobalta-1,3,2,4-dithiadiazole were collected on a Bruker-AXS diffractometer equipped with a SMART APEX CCD, using Mo Kα radiation (λ = 0.71073 Å). The structure was solved by direct methods and refined by full-matrix least-squares methods on F^2. Refinements were performed using SHELXTL (Version 5.10, Bruker-AXS, 1999).

Crystal data for 5-(η^5-cyclopentadienyl)-5-cobalta-1,3,2,4-dithiadiazole: $C_5H_5CoN_2S_2$, M = 216.16, monoclinic, a = 5.8192(15) Å, b = 17.670(6) Å, c = 7.2905(19) Å, β = 105.236(13)°, V = 723.3(4) Å^3, T = 150(2) K, space group $P2_1/c$, Z = 4, D_c = 1.985 g·cm^{-3}, μ(Mo Kα) = 2.861 mm^{-1}, 1779 unique reflections (R_{int} 0.0160) measured. Final R_1[1717 $F \geq 2\sigma(I)$] = 0.0210, wR(all F^2) = 0.0545.

2.3. Calculations. The calculations on $CpCoS_2N_2$ were performed using Gaussian 98[36] and the BRABO package.[37] Geometry optimizations were performed applying standard gradient techniques[38,39] at the density functional (DFT)[40,41] level using the B3LYP functional[42] and the 6-311+G* basis set.[43,44] Initially, the geometry was calculated in C_1 symmetry, introducing nonplanarity in the heterocyclic ring, but the optimization led the structure to a planar conformation. Consequently the symmetry was raised to C_s, the geometry was recalculated, and a frequency calculation was performed

(24) Niu, S. Q.; Hall, M. B. *Chem. Rev.* **2000**, *100*, 353.
(25) Loew, G. H.; Harris, D. L. *Chem. Rev.* **2000**, *100*, 407.
(26) Frenking, G.; Frohlich, N. *Chem. Rev.* **2000**, *100*, 717.
(27) Siegbahn, P. E. M.; Blomberg, M. R. A. *Chem. Rev.* **2000**, *100*, 421.
(28) Blockhuys, F.; Hinchley, S. L.; Marakov, A. Y.; Gatilov, Y. V.; Zibarev, A. V.; Woollins, J. D.; Rankin, D. W. H. *Chem.-Eur. J.* **2001**, *7*, 3592.
(29) Makarov, A. Y.; Bagryanskaya, I. Y.; Blockhuys, F.; Van Alsenoy, C.; Gatilov, Y. V.; Knyazev, V. V.; Maksimov, A. M.; Mikhalina, T. V.; Platonov, V. E.; Shakirov, M. M.; Zibarev, A. V. *Eur. J. Inorg. Chem.* **2003**, 77.
(30) Tersago, K.; Van Droogenbroeck, J.; Van Alsenoy, C.; Herrebout, W. A.; van der Veken, B. J.; Aucott, S. M.; Woolins, J. D.; Blockhuys, F. *Phys. Chem. Chem. Phys.* **2004**, *6*, 5140−5144.
(31) Van Droogenbroeck, J.; Tersago, K.; Van Alsenoy, C.; Aucott, S. M.; Milton, H. L.; Woollins, J. D.; Blockhuys, F. *Eur. J. Inorg. Chem.* **2004**, 3798.
(32) Allen, F. H. *Acta Crystallogr.* **2002**, *B58*, 380.
(33) Boere, R. T.; Klassen, B.; Moock, K. H. *J. Organomet. Chem.* **1994**, *467*, 127.
(34) Granozzi, G.; Casarin, M.; Edelmann, F.; Albright, T. A.; Jemmis, E. D. *Organometallics* **1987**, *6*, 2223.
(35) Edelmann, F. *J. Organomet. Chem.* **1982**, *228*, C47.
(36) Frisch, M. J.; Trucks, G. W.; Schlegel, H. B.; Scuseria, G. E.; Robb, M. A.; Cheeseman, J. R.; Zakrzewski, V. G.; Montgomery, J. J. A.; Stratmann, R. E.; Burant, J. C.; Dapprich, S.; Millam, J. M.; Daniels, A. D.; Kudin, K. N.; Strain, M. C.; Farkas, O.; Tomasi, J.; Barone, V.; Cossi, M.; Cammi, R.; Mennucci, B.; Pomelli, C.; Adamo, C.; Clifford, S.; Ochterski, J.; Petersson, G. A.; Ayala, P. Y.; Cui, Q.; Morokuma, K.; Salvador, P.; Dannenberg, J. J.; Malick, D. K.; Rabuck, A. D.; Raghavachari, K.; Foresman, J. B.; Cioslowski, J.; Ortiz, J. V.; Baboul, A. G.; Stefanov, B. B.; Liu, G. H.; Liashenko, A.; Piskorz, P.; Komaromi, I.; Gomperts, R.; Martin, R. L.; Fox, D. J.; Keith, T.; Al-Laham, M. A.; Peng, C. Y.; Nanayakkara, A.; Challacombe, M.; Gill, P. M. W.; Johnson, B.; Chen, W.; Wong, M. W.; Andres, J. L.; Gonzalez, C.; Head-Gordon, M.; Replogle, E. S.; Pople, J. A.; Gaussian, I., Pittsburgh, PA *Gaussian 98, Revision A.11*; 2001.
(37) Van Alsenoy, C.; Peeters, A. *J. Mol. Struct. (THEOCHEM)* **1993**, *105*, 19.
(38) Pulay, P. *Mol. Phys.* **1969**, *17*, 197.
(39) Pulay, P.; Fogarasi, G.; Pang, F.; Boggs, J. E. *J. Am. Chem. Soc.* **1979**, *101*, 2550.
(40) Hohenberg, P.; Kohn, W. *Phys. Rev.* **1964**, *B136*, 864.
(41) Kohn, W.; Sham, L. J. *Phys. Rev.* **1965**, *A140*, 1133.
(42) Stephens, P. J.; Devlin, F. J.; Chabalowski, C. F.; Frisch, M. J. *J. Phys. Chem.* **1994**, *98*, 11623.
(43) Krishnan, R.; Binkley, J. S.; Seeger, R.; Pople, J. A. *J. Chem. Phys.* **1980**, *72*, 650.
(44) McLean, A. D.; Chandler, G. S. *J. Chem. Phys.* **1980**, *72*, 5639.

to ascertain that the resulting structure was indeed an energy minimum. Chemical shift calculations were performed at the restricted (HF) and unrestricted (UHF) Hartree−Fock[45] and the DFT/B3LYP levels with the 6-31+G* basis set, at the B3LYP/6-311+G* geometry, using the GIAO method implemented in Gaussian 98. Chemical shifts for the carbon and hydrogen atoms were obtained by subtracting the chemical shielding values of these atoms from the ones calculated for tetramethylsilane (TMS), which are 200.7499 and 32.6074 ppm, respectively, at the (U)HF/6-31+G* level, and 191.6496 and 32.1776 ppm, respectively, at the B3LYP/6-31+G* level, also based on a B3LYP/6-311+G* geometry. Chemical shifts for the nitrogen atoms were obtained by subtracting the chemical shielding values of these atoms from the ones calculated for ammonia (NH_3), which are 266.1027 and 263.9129 ppm, respectively, at the (U)HF/6-31+G* and the B3LYP/6-31+G* level, based on a B3LYP/6-311+G* geometry. Chemical shielding factors were calculated at both ring centers (nonweighted mean of the heavy atom coordinates) and at 1 Å above the ring centers to obtain NICS(0)[46] and NICS(1)[47] values, respectively. In addition, the NICS value of free cyclopentadienyl anion was calculated for reasons of comparison: a geometry optimization was performed at the B3LYP/6-311+G* level in D_{5h} symmetry, followed by a chemical shielding calculation at the B3LYP/6-31+G* level. All subsequent calculations of molecular properties were performed at the B3LYP/6-311+G* geometry using that level of theory. Bond orders and atomic valencies were calculated according to the Mayer scheme.[48] Deformation densities were calculated by subtracting the pro-molecular density from the total molecular density. Stockholder charges were calculated as previously reported,[49] based on the Hirshfeld partitioning of space.[50] Atomic dipole moments μ_A were calculated according to $\mu_{A,n} = -\int r_n \Delta\rho_A(\vec{r}) d$, with $n = x$, y, or z, $\vec{r}$ the position vector of the atom, and $\Delta\rho$ the deformation density as usually defined.[51] Fukui functions[52] and local softnesses were calculated by the finite difference approach.[53]

3. Results and Discussion

3.1. Geometry. The molecular framework and atomic numbering of $CpCoS_2N_2$ are shown in Figure 3. Hydrogen atoms are given the same number as the carbon atom they are substituted on. During the geometry optimizations of the C_1 geometry, the structure converted to one in C_s symmetry, with a planar heterocycle and the cyclopentadienyl (Cp) ring eclipsing it. In this arrangement, there are two possible conformers, and consequently a geometry optimization and force-field calculation were performed on both structures. The first, in which one CH unit of the Cp ring eclipses the CoS bond, proved to be an energy minimum for the free molecule. In contrast, the calculation for the C_s form, in which one CH unit eclipses the CoN bond, yielded one imaginary frequency, indicating that the second conformer is a transition state. The energy difference between the two conformers, which is identical to the rotation barrier of the Cp ring, is 0.69 kJ·mol^{-1} at the B3LYP/6-311+G* level. On the basis of this value, the coalescence temperature of the Cp ring can be estimated to be 55 K. Due to the crystal formation, the stacking and the corresponding generation of short contacts between three hydrogen atoms on the cyclopentadienyl ring and S(1), N(2), and N(4) of three neighboring molecules, the symmetry of the molecules in the crystal has been reduced to C_1, with a torsion between both rings of about 8°.

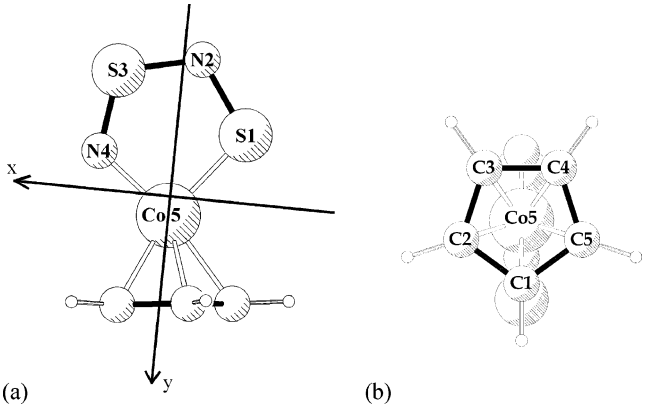

Figure 3. Molecular structure and atomic numbering of $CpCoS_2N_2$. (a) View of the plane of the CoN_2S_2 ring, and (b) view of the plane of the Cp ring.

Table 1. Comparison of Selected Calculated Gas-Phase (r_e in Å and angles in deg) and Experimental Solid-State (r in Å and angles in deg) Geometrical Parameters of $CpCoS_2N_2$

	XRD	B3LYP/6-311+G*
S(1)−N(2)	1.657(2)	1.661
N(2)−S(3)	1.597(2)	1.620
S(3)−N(4)	1.556(1)	1.576
N(4)−Co(5)	1.816(1)	1.804
Co(5)−S(1)	2.0764(6)	2.125
Co(5)−C(1)	2.037(2)	2.084
Co(5)−C(2)	2.042(2)	2.073
Co(5)−C(3)	2.076(2)	2.091
Co(5)−C(4)	2.065(2)	2.091
Co(5)−C(5)	2.044(2)	2.073
C(1)−C(2)	1.417(3)	1.424
C(2)−C(3)	1.419(2)	1.430
C(3)−C(4)	1.409(2)	1.416
C(4)−C(5)	1.413(2)	1.430
C(5)−C(1)	1.420(3)	1.424
S(1)−N(2)−S(3)	111.22(8)	112.45
N(2)−S(3)−N(4)	112.04(7)	110.46
S(3)−N(4)−Co(5)	118.32(8)	119.96
N(4)−Co(5)−S(1)	91.02(5)	90.79
Co(5)−S(1)−N(2)	107.40(5)	106.35

Table 1 presents selected parameters for the calculated gas-phase and the experimental solid-state geometry of $CpCoS_2N_2$. The new determination of the latter, presented in this paper, compares well to the one previously reported.[35] The largest difference in bond lengths between the existing data and our new determination amounts to 0.018 Å for the N(2)−S(3) bond; all other differences are limited to 0.010 Å. From the table, we learn that the B3LYP/6-311+G* data compare very well to the experimental XRD data, keeping in mind that the r_{XRD} are r_α-type distances and that the r_{calc} are r_e distances by definition. The three different SN distances (one shorter, one longer, and one intermediate), which are clear from the experimental data, are convincingly reproduced by the calculation. Even though the differences between theory and experiment regarding the absolute values of the distances are

(45) Fock, V. *Z. Physik.* **1930**, *61*, 126.
(46) Schleyer, P. V.; Maerker, C.; Dransfeld, A.; Jiao, H. J.; Hommes, N. *J. Am. Chem. Soc.* **1996**, *118*, 6317.
(47) Schleyer, P. V.; Manoharan, M.; Wang, Z. X.; Kiran, B.; Jiao, H. J.; Puchta, R.; Hommes, N. *Org. Lett.* **2001**, *3*, 2465.
(48) Mayer, I. *Chem. Phys. Lett.* **1983**, *97*, 270.
(49) Rousseau, B.; Peeters, A.; Van Alsenoy, C. *Chem. Phys. Lett.* **2000**, *324*, 189.
(50) Hirshfeld, F. L. *Theor. Chim. Acta* **1977**, *44*, 129.
(51) De Proft, F.; Van Alsenoy, C.; Peeters, A.; Langenaeker, W.; Geerlings, P. *J. Comput. Chem.* **2002**, *23*, 1198.
(52) Parr, R. G.; Yang, W. T. *J. Am. Chem. Soc.* **1984**, *106*, 4049.
(53) Geerlings, P.; De Proft, F.; Langenaeker, W. *Chem. Rev.* **2003**, *103*, 1793.

Table 2. NMR Chemical Shifts (ppm) for $CpCoS_2N_2$, Relative to TMS for Carbon and Hydrogen and to NH_3 for Nitrogen[a]

	RHF 6-31+G*	UHF 6-31+G*	B3LYP 6-31+G*	expt
C(1)	165.49	83.10	77.08	
C(2)/C(5)	249.18	68.45	75.27	
C(3)/C(4)	200.17	76.17	80.25	
average	212.84	74.47	77.62	82.86
H(1)	12.29	7.34	5.83	
H(2)/H(5)	14.03	7.34	4.15	
H(3)/H(4)	10.87	5.21	5.15	
average	12.42	6.48	4.87	5.67
N(2)	748	414	521	431
N(4)	842	481	673	550

[a] For further details, see text.

debatable, the trends are unequivocal; the correct description of these bonds is crucial for the rest of this work when the bonding and aromaticity of $CpCoS_2N_2$ are discussed (section 3.4). A final feature of the geometry of this compound is the Co−Cp distance, which is expressed by the CoC distances, and again the DFT results correspond well to the solid-state results. This confirms the findings of previous studies[28,31] which showed that the B3LYP/6-311+G* combination performs quite well for systems containing an NSNS fragment in a ring.

The bond lengths of the three NS bonds are of particular interest. In the nonorganometallic analogue 1,3$\lambda^4\delta^2$,2,4-benzodithiadiazine, four of the π-electrons in the heterocycle are localized in two of the NS bonds.[28] This is based on the fact that one long [1.697(5) Å] and two short [1.548(3) and 1.543(3) Å] distances were found in the experimental determination of the gas-phase geometry by electron diffraction.[28] High-level theoretical calculations of the gas-phase structure and measurements of the solid-state structure confirmed this fact, as did studies on a large number of fluoro-substituted derivatives of 1,3$\lambda^4\delta^2$,2,4-benzodithiadiazine.[29] For $CpCoS_2N_2$, this is not the case. Here, one shorter, one longer, and one intermediate bond length are obtained from both the calculations and the experiment. Since it is known that the heterocycle in 1,3$\lambda^4\delta^2$,2,4-benzodithiadiazine is anti-aromatic and that this can be linked to the localization of double bonds, a similar reasoning—based only on these geometrical issues—would lead to the prediction that the heterocycle in $CpCoS_2N_2$ is less anti-aromatic or perhaps even aromatic. This will be discussed in greater detail below (section 3.4).

3.2. NMR Parameters. Chemical shift values, calculated at the Hartree−Fock level, are often reasonably accurate— for organic molecules sometimes even more accurate than the corresponding DFT shifts. For more complex systems, however, electron correlation has to be taken into account (see for example ref 54). Thus, in the case of the organometallic compound under investigation, chemical shifts were calculated at both levels. The values of the NMR chemical shifts for the carbon and hydrogen atoms of $CpCoN_2S_2$ were calculated as the average of the five respective values without weighting due to the very low rotation barrier of the Cp ring. They have been listed in Table 2 referenced to tetramethylsilane (TMS). The experimental values for nitrogen, referenced to (liquid) ammonia (NH_3), have been taken from ref 33 and have also been listed in Table 2. The experimental chemical shift values of the carbon and hydrogen atoms we report here, recorded in $CDCl_3$, compare well to the ones published previously.[34,35]

The table shows that the NMR parameters calculated at the RHF level are unrealistic since the calculation grossly overestimates the chemical shift values for all nuclei. The spread in the values of the carbon atoms (more than 80 ppm) is striking, and a similar effect is seen for the hydrogen shifts. This is most likely due to the poor quality of the wave function at this level of theory for these types of organometallic compounds. As problems with the instability of the wave function are well-known in the field of compounds containing multiple SN bonds, we investigated this issue further by testing the wave function for possible Hartree−Fock instabilities at the B3LYP/6-311+G* geometry. The wave function was indeed found to be unstable. Therefore, the chemical shieldings were recalculated at the unrestricted Hartree−Fock (UHF) level and the corresponding chemical shift values were obtained by subtracting them from the RHF-calculated shieldings of the reference compounds, the latter having stable wave functions. From the UHF results in Table 2, it is clear that it is indeed the instability that causes the unrealistic NMR results. Thus, the UHF parameters correspond quite well to the experimental ones.

The values for the carbon atoms are of similar quality for UHF and DFT. Thus, the average shift values are 74.5 and 77.6 ppm, respectively, and can be directly compared to the experimental value of 82.9 ppm. For the hydrogen shifts, we see that the calculated average chemical shift at the UHF level (6.48 ppm) overestimates the experimental value (5.67 ppm) by an amount equal to the one by which B3LYP (4.87 ppm) underestimates it. Finally, for both nitrogen shifts we see that both methodologies show large differences with the experimental values, but it is known from previous studies that this is not unusual.[29,30] However, the assignment of the signal at 550 ppm, which is broader due to coupling with the nuclear spin of the cobalt atom, to N(4), can now be confirmed by both computational methods.

Table 3. Calculated Atomic Stockholder Charges (in $|e|$) for $CpCoS_2N_2$

	stockholder
S(1)	0.012
N(2)	−0.197
S(3)	0.219
N(4)	−0.206
Co(5)	0.001
C(1)	−0.038
C(2)/C(5)	−0.026
C(3)/C(4)	−0.024
H(1)	0.070
H(2)/H(5)	0.073
H(3)/H(4)	0.075

3.3. Charge and Dipole Analysis. The stockholder charges of $CpCoS_2N_2$ have been compiled in Table 3. Their analysis yields a total charge in the cyclopentadienyl ring of 0.231 $|e|$ and this is naturally equal and opposite to the charge in the metalloheterocyclic five-membered ring. In the latter, the charge is completely situated in the NSNS fragment. Thus, the charge on the cobalt atom is zero, the nitrogen atoms have a

(54) Magyarfalvi, G.; Pulay, P. *J. Chem. Phys.* **2003**, *119*, 1350.

Table 4. Components $\mu_{A,n}$ of the Atomic Dipole Moment Vectors μ_A, Components $q_A \cdot R_{A,n}$ of the Atomic Charge Transfers, and Components μ_n of the Total Molecular Dipole Moment μ, in au, Calculated for $CpCoS_2N_2$[a]

	$\mu_{A,x}$	$\mu_{A,y}$	$\mu_{A,z}$	$q_A \cdot R_{A,x}$	$q_A \cdot R_{A,y}$	$q_A \cdot R_{A,z}$
S(1)	0.006	−0.065	0.000	−0.030	−0.029	0.000
N(2)	0.094	0.273	0.000	0.132	0.990	0.000
S(3)	−0.046	0.025	0.000	0.506	−0.949	0.000
N(4)	−0.124	−0.132	0.000	−0.720	0.369	0.000
Co(5)	−0.004	0.157	0.000	0.000	0.001	0.000
C(1)	−0.127	0.049	0.000	0.098	−0.137	0.000
C(2)	−0.038	0.057	−0.122	0.026	−0.096	0.055
C(3)	0.095	0.059	−0.077	−0.036	−0.097	0.032
C(4)	0.095	0.059	0.077	−0.036	−0.097	−0.032
C(5)	−0.038	0.057	0.122	0.026	−0.096	−0.055
H(1)	−0.152	−0.020	0.000	−0.326	0.236	0.000
H(2)	−0.045	−0.012	−0.148	−0.120	0.265	−0.300
H(3)	0.126	0.002	−0.091	0.239	0.312	−0.191
H(4)	0.126	0.002	0.091	0.239	0.312	0.191
H(5)	−0.045	−0.012	0.148	−0.120	0.265	0.300
sum	−0.076	0.500	0.000	−0.120	1.249	0.000
sum (D)	−0.193	1.271	0.000	−0.305	3.175	0.000
μ_x	−0.196					
μ_y	1.749					
μ_z	0.000					
μ	1.760					
μ_x (D)	−0.498					
μ_y (D)	4.446					
μ_z (D)	0.000					
μ (D)	4.474					

[a] Important values have also been given in D.

negative charge, and positive charges are located on the sulfur atoms.

The molecular dipole moment, μ, was calculated to be 4.474 D, and its components are $\mu_x = -0.499$ D and $\mu_y = -4.446$ D, in the axis system given in Figure 3. The nth component of the molecular dipole, μ_n with $n = x, y, z$, can be written as

$$\mu_n = \sum_A q_A R_{A,n} + \sum_A \mu_{A,n}$$

which is the sum of the contributions of charge transfer (first term, with q_A the stockholder charge and $R_{A,n}$ the coordinate of atom A) and of the intra-atomic charge polarization, calculated by the atomic dipole moment components $\mu_{A,n}$ (second term). Table 4 compiles these components.

Figure 3 indicates that the vector connecting the centers of both rings is almost parallel to the y-axis. The total molecular dipole moment vector too is almost parallel to the y-axis, and this can be explained by the fact that the net charges of both rings, which are equal but of opposite sign, are spatially separated mainly along the y-axis as well. A closer look at the heterocycle shows that N(2) and S(3) have a similar but opposite stockholder charge (Table 3). Because of their symmetrical positions relative to the y-axis, the large y-components of the charge-transfer contributions of both atoms (0.990 and −0.949 au, respectively) cancel each other. In a certain sense, symmetrical relative positions can also be found for S(1) and N(4), but the absolute value of the charge on N(4) is much larger than the one on S(1) (Table 3). Thus, a net positive charge-transfer contribution in the y-direction is obtained for the heterocycle taking into account the zero charge on the cobalt atom. When the same is done for the cyclopentadienyl ring, a net positive of the charge-transfer contribution along the y-axis is obtained for this ring. This is due to the systematically larger positive charge values of the hydrogen atoms compared to the negative charge values of the carbon atoms on which they are substituted. A similar reasoning can be applied to the x-component of the charge transfer, which is mainly due to the heterocycle, but considerably smaller than the y-component.

Table 5. NICS(0) and NICS(1) Values in ppm for Both Rings in $CpCoS_2N_2$ and for an Isolated Cp Ring, Calculated at the B3LYP/6-31+G*//B3LYP/6-311+G* Level

		$CpCoS_2N_2$	Cp
CoS_2N_2	NICS(0)	−19.73	
	NICS(1)	−18.16	
Cp	NICS(0)	−32.47	−12.63
	NICS(1)	−12.67	−9.41

Turning our attention to the atomic dipoles, the contributions of the strongly polarized NSNS fragment sum up to −0.070 and 0.101 au (−0.177 and 0.257 D) in the x- and y-directions, respectively. The cobalt atom is polarized along the vector connecting the charge centers of both rings, since its μ_x is negligible. Finally, for the atoms of the cyclopentadienyl ring a net atomic dipole contribution of 0.241 au (0.613 D) is found in the y-direction, due to the presence of the heterocyclic ring; the contributions in the x-direction sum up to a negligible −0.003 au.

3.4. Aromaticity and Bonding. Despite the difficulties encountered when defining powerful aromaticity criteria on one hand and understanding the precise nature of aromaticity[55] on the other, we believe that we have presented an acceptable way to describe the aromaticity of NSNS-containing compounds in a previous study.[31] In the past few years, relatively minor attention has been paid to the aromatic properties of the chelate metallacycles of organometallic compounds in particular, called metalloaromaticity.[56] In this study, we will combine magnetic and a number of structural criteria for the description of the (anti-/non-)aromaticity of $CpCoS_2N_2$.

Starting with the magnetic criteria, the results of the calculation of the NICS(0) values are given in Table 5: these are negative for both rings, indicating aromaticity for the Cp ring and the heterocycle. It was pointed out by Schleyer et al.[47] that there are some artifacts in the NICS(0) values, calculated in the plane of the molecule, due to the σ-framework of the molecule. To circumvent this, they proposed to calculate so-called NICS(1) values at 1 Å above the ring center, since aromaticity involves the delocalization of the π-electrons. For the metalloheterocycle and the cyclopentadienyl ring, NICS(1) values of −18.16 and −12.67 ppm are found, respectively. It is clear that both rings are indeed aromatic. The heterocycle has an absolute NICS value not uncommon for five-membered rings. For the cyclopentadienyl ring in $CpCoS_2N_2$, a quite large NICS(0) value was found (−32.5 ppm) and a much smaller corresponding NICS(1) value. For reasons of comparison, we calculated

(55) Minkin, V. I.; Glukhovsev, M. N.; Simkin, B. Y. *Aromaticity and Antiaromaticity*; John Wiley & Sons: New York, 1994.
(56) Masui, H. *Coord. Chem. Rev.* **2001**, *219*, 957.

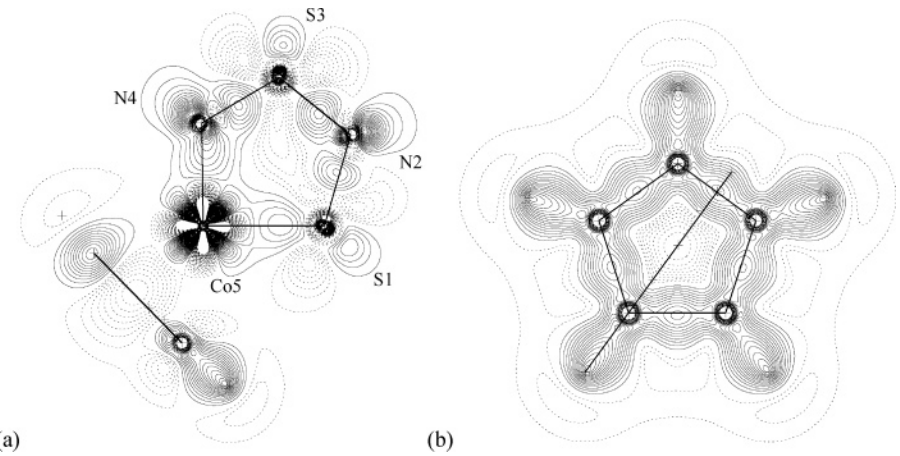

Figure 4. Calculated deformation density maps of $CpCoS_2N_2$. (a) Density in the plane of the heterocycle ring, and (b) density in the plane of the Cp ring. Full lines indicate positive electron density, dashed lines negative electron density, and [-·-] zero electron density.

the NICS values of free cyclopentadienyl anion, and these are also given in Table 5. We see that the Cp ring in $CpCoS_2N_2$ has an increased aromaticity compared to the free ligand, which has NICS(0) and NICS(1) values of only −12.63 and −9.41 ppm, respectively. This considerable difference between the values of free and ligated cyclopentadienyl anion may be due to the interference of the magnetic fields of both rings (which are almost perpendicular to one another), caused by their ring currents, which makes a quantitative interpretation of the values difficult. Still, the NICS values suggest quite strongly that both rings in $CpCoS_2N_2$ are aromatic. Both the chelation of a highly reactive fragment like $(SN)_x$ leading to a stabilized ring and the formation of an aromatic η-bound complex are examples of metalloaromaticity. $CpCoS_2N_2$ can thus be seen as a metalloaromatic compound.

The aromaticity of the CoS_2N_2 ring, obtained from the above-mentioned magnetic criterion, is in line with the prediction based on the delocalization of π-electrons in the system, as suggested by the geometrical data presented in section 3.1. We will now discuss these structural criteria in greater detail by means of bond lengths, bond orders, and deformation densities. Figure 4 shows the calculated deformation densities in the planes of the CoS_2N_2 and the Cp ring. Figure 4b shows that in the Cp ring the electron density is evenly distributed over the entire ring. This points to full electron delocalization and is in correspondence with the suggested aromaticity. For the heterocycle (Figure 4a), it is not so straightforward to conclude aromaticity from the deformation density map. The qualitative view of the figure, however, is in good accordance with the one that was found for the aromatic 5-oxo-1,3,2,4-dithiadiazole (Roesky's ketone), OCS_2N_2.[31] The electron distribution around the cobalt atom is spread over both the CoN and the CoS bonds, and the contribution of the d-orbitals of the metal in the bond formation can be clearly seen in the figure.

Table 6 presents the Mayer bond orders and the valencies of all atoms in $CpCoS_2N_2$. The bond orders in the cyclopentadienyl fragment have the expected values: the perfect delocalization of the electrons over the CC bonds results in bond orders of about 1.5 and the CH bonds have the usual bond order of about 1. Similar conclusions can be drawn from the values of the valencies. The overall conclusion for the Cp ring is that C(1) is bound more strongly to Co than C(2) and C(5), which in turn are bound more strongly to the metal than C(3) and C(4). For the heterocycle the values are less easily understood. Thus, the NS bond length sequence of the three clearly different values (1.661, 1.620, and 1.576 Å) is not at all expressed in the bond orders (0.9, 1.1, and 1.0 for the same bonds). Yet, a similar situation was found in the study of the aromatic 5-oxo-1,3,2,4-dithiadiazole (Roesky's ketone) and its constitutional isomers. It seems that when the bond orders of the three NS bonds are almost equal, this can also be an indication of electron delocalization and aromaticity.[31] In contrast, the valencies of the atoms in the heterocycle do present a clearer picture of the bonding in this ring. Thus, the values indicate a single bond between S(1) and N(2), an intermediate bond between N(2) and S(3), and a quasi-double bond between S(3) and N(4). This is in complete agreement with the geometrical data. The apparent disagreement between bond order and valency data is mainly due to the fact that the Mayer bond orders are calculated in terms of atomic orbitals. As a consequence, nonzero terms between noncovalently bound atoms will appear, especially when heavy atoms are involved (see ref 57 and references therein). For this reason, in the case of $CpCoS_2N_2$, values are obtained

Table 6. Calculated Mayer Bond Orders and Valencies of the Atoms in $CpCoS_2N_2$

	BO		valency
S(1)−N(2)	0.9	S(1)	2.1
N(2)−S(3)	1.1	N(2)	2.4
S(3)−N(4)	1.0	S(3)	2.5
N(4)−Co(5)	1.5	N(4)	2.7
Co(5)−S(1)	0.8	Co(5)	4.5
Co(5)−C(1)	0.5	C(1)	4.7
Co(5)−C(2)	0.4	C(2),C(5)	4.4
Co(5)−C(3)	0.3	C(3),C(4)	4.3
Co(5)−C(4)	0.3	H(1)	0.9
Co(5)−C(5)	0.4	H(2),H(5)	0.9
C(1)−C(2)	1.5	H(3),H(4)	0.9
C(1)−C(5)	1.5		
C(2)−C(3)	1.4		
C(4)−C(5)	1.4		
C(3)−C(4)	1.5		
C−H	0.9		

(57) Bridgeman, A. J.; Cavigliasso, G.; Ireland, L. R.; Rothery, J. *J. Chem. Soc., Dalton Trans.* **2001**, 2095.

Table 7. Fukui Functions f^+ and f^- and Local Softnesses s^+ and s^- of the Different Atoms in $CpCoS_2N_2$

	f^+	f^-	s^+	s^-
S(1)	0.191	0.136	0.804	0.574
N(2)	0.090	0.113	0.379	0.477
S(3)	0.144	0.154	0.608	0.647
N(4)	0.069	0.134	0.289	0.566
Co(5)	0.077	0.096	0.326	0.403
C(1)	0.037	0.046	0.154	0.194
C(2)/C(5)	0.064	0.049	0.268	0.205
C(3)/C(4)	0.050	0.042	0.209	0.175
H(1)	0.028	0.028	0.118	0.117
H(2)/H(5)	0.036	0.029	0.154	0.123
H(3)/H(4)	0.032	0.027	0.136	0.112

that are sometimes not easily interpreted. The valencies, on the other hand, are calculated by summing up all bond orders of a given atom, and this quantity is thus usually a more useful measure of the total number of electrons that the given atom uses for bond formation.

Finally, we want to rationalize which of the suggested bonding models in Figure 2 best fits the structural results found for $CpCoS_2N_2$. The delocalization of the electrons in the NSNS fragment has been convincingly shown. We will now take a closer look at the CoS and CoN bonds. The bond orders suggest that the CoN bond has partial double bond character. We do not find this for the CoS bond, but, as already mentioned, an underestimation of the bond strength by the bond order is not uncommon. Therefore, it is useful to compare the present CoS bond length with a number of 'reference bond lengths' in analogous components. Recently, some structural work has been performed on (η^5-cyclopentadienyl)cobaltadithiolene rings.[58−63] These systems are known to be aromatic and resemble $CpCoS_2N_2$ very well in the sense that a Co^{III} atom is coordinatively saturated, is itself involved in an aromatic ring, and is bound to a η^5-cyclopentadienyl ring. The results of solid-state structure determinations by XRD[58,59,61] produce CoS distances between 2.10 and 2.13 Å. The conclusion for the CoS bond length of 2.0764(6) Å in $CpCoS_2N_2$ is that it must have partial double bond character as well. From these findings, we conclude that the bonding model with a complete delocalization in the heterocycle gives the correct description of the structure of $CpCoS_2N_2$ as a five-membered aromatic ring.

3.5. Reactivity Sites. After having described the global bonding and reactivity/aromaticity of $CpCoS_2N_2$, we finally turn our attention to the local reactivity description. The values of the Fukui functions and softnesses are given in Table 7. To find the most suitable sites for attack by a given reagent, it is known that condensed Fukui functions and atomic charges are good descriptors when considering soft and hard reagents, respectively. For all details on these functions we refer to a recent review.[53] We mention here that a maximum value of the Fukui function f^+ and local softness s^+ (or f^- and s^-) indicates the most suitable place toward nucleophilic (or electrophilic) attack by a soft reagent.

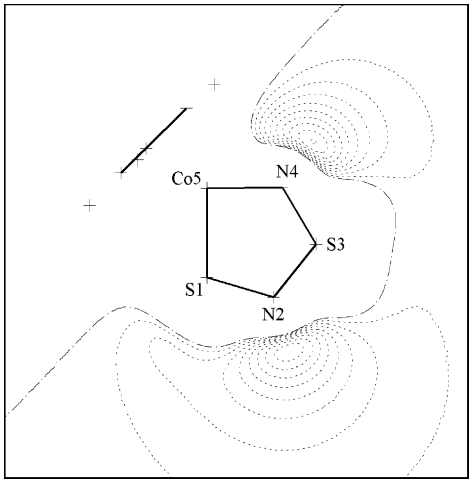

Figure 5. Molecular electrostatic potential map in the plane of the CoS_2N_2 ring. Crosses + indicate the projections of the atoms in the plane. White areas depict positive potentials, [-•-] gives the zero isopotential line, and negative isopotentials are indicated by the dotted lines.

The most likely site for an orbital-controlled (based on the Fukui functions) nucleophilic attack in $CpCoS_2N_2$ is S(1), but, in view of its very small positive charge (Table 3), one would not expect a charge-controlled nucleophilic attack to take place on this atom. Rather, S(3) is the favored site for a charge-controlled nucleophilic attack, but it is a less likely site for an orbital-controlled nucleophilic reaction. Conversely, for an electrophilic attack, S(3) is the most likely place, even though, due to its positive charge, a charge-controlled electrophilic attack cannot take place on that site. The question of which site in $CpCoS_2N_2$ *is* favored for a charge-controlled electrophilic attack can be answered in the following way. The next highest value of f^- in Table 7 is found for S(1), but again this site is disfavored for a charge-controlled electrophilic attack due to its positive atomic charge, even if this is very small. Just below the value of S(1) we find N(4), and, even though it has a lower local softness value for electrophilic attack than both sulfur atoms, it has a pronounced negative charge (the largest negative charge in the molecule) and is therefore the most likely site for a charge-controlled attack by a hard electrophile.

After this general reactivity description and as an example of a charge-controlled attack by a hard electrophile, we will focus our attention on the protonation of the heterocycle. A reaction with a hard electrophile like H^+ will be charge-controlled and will take place at a negatively charged site, i.e., at a nitrogen atom. We will now study a protonation reaction taking place at both nitrogen atoms from a kinetic and thermodynamic point of view.

For the discussion on kinetics we will use a plot of the molecular electrostatic potentials (MEP), which is given in Figure 5. Per definition, the MEP is the potential felt by a unit positive charge when it approaches the molecule, and thus negative areas depict the path of approach of an electrophilic species. Figure

(58) Armstrong, E. M.; Austerberry, M. S.; Beddoes, R. L.; Helliwell, M.; Joule, J. A.; Garner, C. D. *Acta Crystallogr.* **1993**, *C49*, 1764.
(59) Fourmigue, M.; Perrocheau, V. *Acta Crystallogr.* **1997**, *C53*, 1213.
(60) Nomura, M.; Takayama, C.; Sugiyama, T.; Yokoyama, Y.; Kajitani, M. *Organometallics* **2004**, *23*, 1305.
(61) Takayama, C.; Kajitani, M.; Sugiyama, T.; Sugimori, A. *J. Organomet. Chem.* **1998**, *563*, 161.
(62) Takayama, C.; Takeuchi, K.; Ohkoshi, S.; Janairo, G. C.; Sugiyama, T.; Kajitani, M.; Sugimori, A. *Organometallics* **1999**, *18*, 2843.
(63) Won, J. H.; Kim, D. H.; Kim, B. Y.; Kim, S. J.; Lee, C.; Cho, S.; Ko, J.; Kang, S. O. *Organometallics* **2002**, *21*, 1443.

5 shows the MEP in the plane of the CoS_2N_2 ring in which only the negative isopotential lines have been drawn. Two clear potential minima can be seen near both nitrogen atoms, originating from the lone pairs on these atoms. The minima at both sulfur atoms are a lot shallower and disappear into the minima due to the nitrogen atoms. The minimum at N(4) ($V_{min.} = -0.088$ au) is slightly deeper than the one at N(2) ($V_{min.} = -0.086$ au), but the difference is very small, which corresponds quite well with the values of the charges on both atoms (Table 3). This means that under *kinetic* conditions both sites will be equally accessible to electrophiles and in the case of H^+ both nitrogen atoms will be protonated to an equal amount. Under *thermodynamic* conditions, however, the situation is completely different. The energy difference between $CpCoS_2N_2$ protonated on N(2) and $CpCoS_2N_2$ protonated on N(4) is 43.66 kJ·mol^{-1} in favor of the latter. Thus, when protonation is carried out under thermodynamic conditions, e.g., at room temperature, only substitution on N(4) will be observed.

4. Conclusions

5-(η^5-Cyclopentadienyl)-5-cobalta-1,3,2,4-dithiadiazole was synthesized and its structure redetermined experimentally by single-crystal X-ray diffraction. The experimental molecular geometry was compared to the B3LYP/6-311+G* geometry of the isolated molecule, and a good agreement was found. Further molecular and atomic properties were calculated at this level to obtain insight in the structure, aromaticity, and reactivity of the title compound. Observed trends in NMR parameters of the title compound were theoretically predicted based on calculated NMR shielding constants. Wave function instability problems were dealt with. The Hirshfeld partitioning of the electron density was used to calculate the atomic charges and dipoles, which directly led to the understanding of the origin of the molecular dipole. A consistent combination of magnetic and structural criteria confirmed that both rings are aromatic. Finally, a number of reactivity descriptors from conceptual DFT together with stockholder charges were calculated and the reactive sites within the molecule could be identified. The protonation of the heterocyclic ring was studied in greater detail making use of some additional quantities such as energies of protonated isomers and molecular electrostatic potentials.

Acknowledgment. J.V.D. thanks the Flemish governmental institution IWT for a pre-doctoral grant. A.D.H. thanks the National Science Foundation for partial support of this project in the form of grant 0086313, Youngstown State University for 2000−2001 sabbatical support, and Bruker-Nonius for collecting the preliminary diffraction data on the title complex. F.B. and C.V.A. gratefully acknowledge support by the University of Antwerp under BOF UA/SFO UIA 2002. The authors are grateful to Prof. Frank De Proft of the University of Brussels (VUB) for the interesting and useful discussions on conceptual DFT.

Supporting Information Available: Crystallographic information in the form of a CIF file, containing the atomic coordinates, the molecular geometry, and ADPs for $CpCoS_2N_2$. This material is available free of charge via the Internet at http://pubs.acs.org.

OM0494059